Looking underneath fullerenes on Au(110): Formation of dimples in the substrate

M. Hinterstein,[1,2] X. Torrelles,[1,*] R. Felici,[3] J. Rius,[1] M. Huang,[4] S. Fabris,[4] H. Fuess,[2] and M. Pedio[5]
[1]*Institut de Ciència de Materials de Barcelona, ICMAB-CSIC, 08193 Barcelona, Spain*
[2]*Technische Universität Darmstadt, 64277 Darmstadt, Germany*
[3]*European Synchrotron Radiation Facility (ESRF), 38043 Grenoble, France*
[4]*INFM-CNR DEMOCRITOS Theory@Elettra Group and SISSA, 34014 Trieste, Italy*
[5]*TASC National Laboratory, INFM-CNR, 34012 Trieste, Italy*
(Received 30 January 2008; published 30 April 2008)

The adsorption of organic molecules on metal surfaces can lead to complex nanostructuration of the supporting substrate. The precise atomistic and electronic structures of the C60/Au(110) interface are unveiled by combining synchrotron-based diffraction and spectroscopic techniques with density functional theory calculations. We show that the interaction between C60 molecules with Au(110) surface induces a massive interface reorganization, which leads to the Au(110)-$p(6\times5)$ substrate reconstruction and to the formation of surface nanodimples. The fullerenes are hosted by these nanodimples, which are one and two layers deep. We provide evidence that the larger contact area between the C60 and the metal, which results from the substrate rearrangement, allows for the formation of strong directional C-Au bonds.

DOI: 10.1103/PhysRevB.77.153412 PACS number(s): 68.35.bd, 61.05.cp, 68.35.bp, 68.65.Cd

The development of methods capable of producing ordered surface nanostructures based on the self-assembly of large molecules (LMs) is a stimulating field for many technological applications. The chemical and physical properties of surface-supported nanostructures can, in principle, be tailored by functionalizing the molecular building blocks confined to two-dimensional systems.[1,2] Exploiting LMs for the fabrication of surface-supported functional nanostructures requires the understanding and the characterization of the structural and electronic properties of the molecular-surface interface, at a level which is presently unavailable for many relevant systems. This is particularly important when the interface structure is strongly modified by the molecular interaction[3] and, as in the case of large molecular adsorbates, when the details of the interface are very difficult to access with standard surface science techniques.[4]

The mechanisms of LM surface anchoring can be quite complex due to a balance of intermolecular binding forces and of molecule-substrate interaction involving a large number of sites. In this context, the interaction of fullerenes with surfaces can be seen as a model system. The presence of strong directional π molecular states, together with the capability of being an acceptor or donor of electrons, allows fullerene to establish different kinds of interaction, ranging from van der Waals to ionic and to covalent bonding, through the C atoms that are in direct contact with the substrate.

The majority of studies of fullerenes interacting with surfaces are based on scanning tunneling microscopy (STM) measurements on systems ranging from isolated molecules up to ordered supramolecular assemblies.[5,6] However, the structural and binding features of the contact region are not directly accessible by STM since this technique images the surface electron density of states, which, in the case of LMs, is in general not very sensitive to the buried interface structure.[4] This lack of information on the substrate reorganization induced by adsorbates strongly limits the full comprehension of these systems. For this reason, STM is often combined with density functional theory (DFT) calculations to get information on the atomic and electronic structures of the interface. In turn, these calculations rely on a substrate atomic model, which is usually not known and it is implicitly assumed to be either the unreconstructed substrate surface, or the reconstructed surface observed upon molecular desorption, or some simple model proposed on the basis of STM images.[4,7]

In this study, we have first determined the detailed structure of the C60-substrate interface with surface x-ray diffraction (SXRD)[8,9] and the DFT calculations have then been performed on the resulting interface structure. By comparing experimental SXRD, photoemission (PE), and inverse photoemission (IPE) data with DFT calculations, we unveil the strong surface reconstruction at the metal-fullerene interface, which leads to the formation of nanoscopic dimples (nanodimples) in the substrate and allows the formation of a characteristic directional bond in the contact region. The driving force for this surface reorganization is provided by the strong hybridization between the molecular π orbitals and the surface *s* metal states, which is maximized by the binding larger contact region available for fullerenes in the nanodimples.

SXRD is a powerful technique capable of accessing structures of surfaces and interfaces at atomic resolution and is used to determine molecular surface arrangements on metals and semiconductor substrates.[3,10–12] The first structural model proposing a fullerene ordering mechanism involving major surface reconstruction was proposed for the C_{60}/Au(110) system using in-plane SXRD data.[3] Electron energy loss spectroscopy estimated a charge transfer at the interface of 1 ± 1 electron/molecule, which indicates strong involvement of the substrate into bond formation with the C60 cage but the large experimental uncertainty prevents a detailed understanding of the bonding.[13] The interpretation that adsorbed fullerenes can accommodate into surface defects produced in the topmost substrate layers by surface metal atom displacement is now well established,[10,14] but a clear description of these defects, and thus of the contact area, is missing.

By a full three-dimensional (3D) SXRD analysis, we have determined the interface structure, which results from sub-

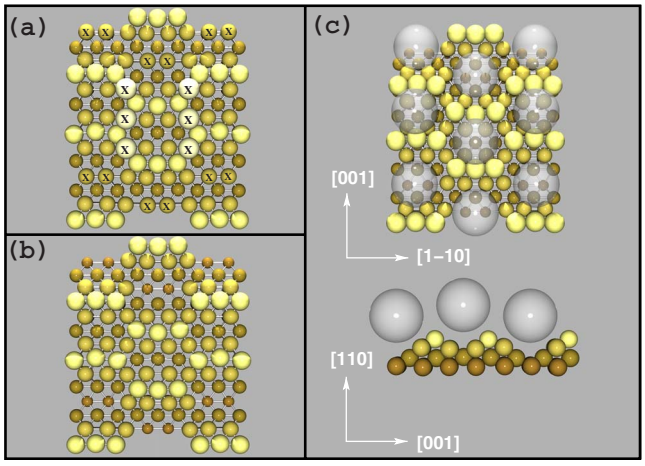

FIG. 1. (Color online) (a) Initial model for LS refinement based on Ref. 3. Darker atom tonalities refer to deeper atoms from the surface. (b) Optimized interface structure: Best fit is obtained when suppressing some gold atoms (marked with X) from the initial model. (c) Top and lateral views of the C_{60}/Au(110)-$p(6\times5)$ interface structure. The transparent spheres simulating the C60 molecules indicate absence of preferential orientation.

strate reorganization upon fullerene adsorption on Au(110). The sample was prepared, as already described in Refs. 13 and 15–17 with similar surface quality.[3] Data were collected at beam lines ID03 and ID32 of the European Synchrotron Radiation Facility (ESRF) in Grenoble[18,19] (beam energy: 13.4 keV for both experiments). A total of 1096 reflections, specific to the $p(6\times5)$ structure, were measured. These are reduced to 834 after averaging between the equivalent reflections with symmetry $p2mg$,[9] which form part of 48 fractional order rods (FORs) and 8 crystal truncation rods (CTRs). The good quality of the sample formed by continuous and homogeneous domains is reflected in the negligible surface roughness, the domain size of nearly 2000 Å, and the refined coverage fraction of 0.98.

The 3D starting model was obtained by out-of-plane expanding the published projected model of Fig. 1(a).[3] The atoms marked with the symbol "X" were suppressed from the model after refining their population coefficients by means of least-squares (LS) refinement procedures. The resulting model can be visualized in Fig. 1(b) consisting in 188 gold atoms distributed over 7 layers and four adsorbed fullerene molecules and where the marked atoms were no longer present (i.e., 6 from the topmost layer and 4 from the third layer). The interface structure was determined by refining the positions of the gold atoms (146 parameters) and those of the fullerene molecules (4 parameters) plus 3 thermal vibration parameters (1 for the fullerenes, 1 for the first layer gold atoms, and 1 for the remaining gold atoms).

The optimized model structure is shown in Fig. 1(c) and involves only the four outermost substrate layers. The refined 3D model presents two nonequivalent nanopits per unit cell, each hosting a fullerene molecule, and being one and two layers deep. This results in a difference in the two fullerene heights of about 1.2(2) Å, close to the corrugation of 1 Å proposed by Gimzewski *et al.*[20] The experimental data are not sensitive to the orientation of the molecule. Its rotating

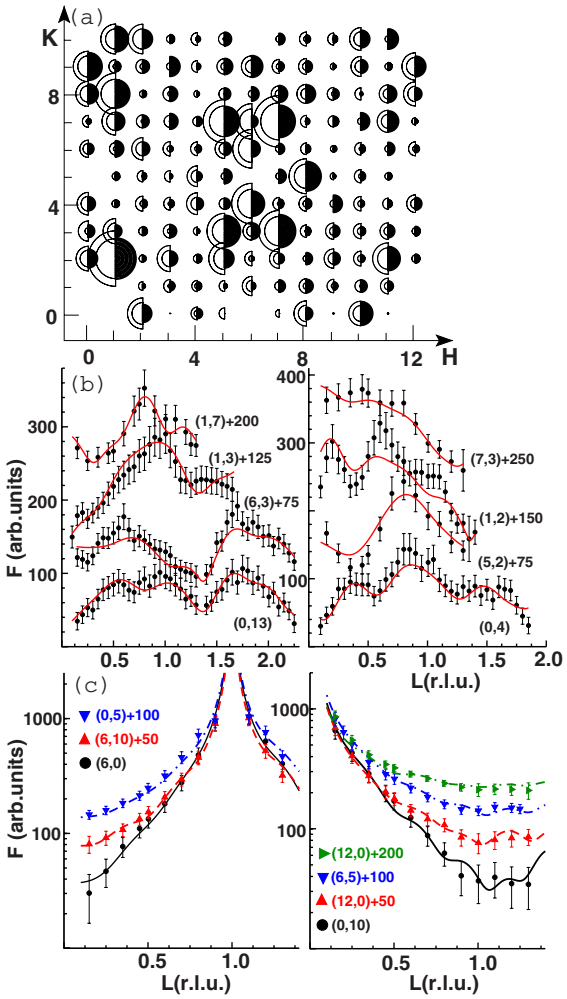

FIG. 2. (Color online) (a) Experimental and calculated in-plane data of the C_{60}/Au(110)-$p(6\times5)$ surface reconstruction. Measured values and their associated uncertainties are proportional to the radii of the two empty semicircles. Filled semicircles are proportional to calculated values obtained from the final structure model shown in Fig. 1(c). [(b) and (c)] Experimental (dots) and calculated (continuous lines) data for several fractional order (b) and crystal truncation rods (c) from final structure (values close to the curves indicate their corresponding offset for better visualization).

nature is experimentally supported by the high carbon Debye–Waller values (B_C=80 Å^2) obtained from the refinement procedure, which indicate strong positional disorder of the C atoms in the molecule.[15]

The final reduced χ^2 of the least-squares refinement is 1.0. Experimental SXRD data (filled semicircles) are shown in Fig. 2 and compared to calculated values for the optimized model (continuous lines).

There are two symmetry-independent nanopits in the model, the number of gold atoms and the local environment around each fullerene is similar (19 and 18 gold atoms).

The closest Au-Au bond length in the bulk material is 2.88 Å, the shortest and longest being 2.57(3) Å and 3.19(3) Å, respectively. The minimum value represents a bond contraction of 11% that has been observed in similar systems.[21] The larger distortions correspond to atomic dis-

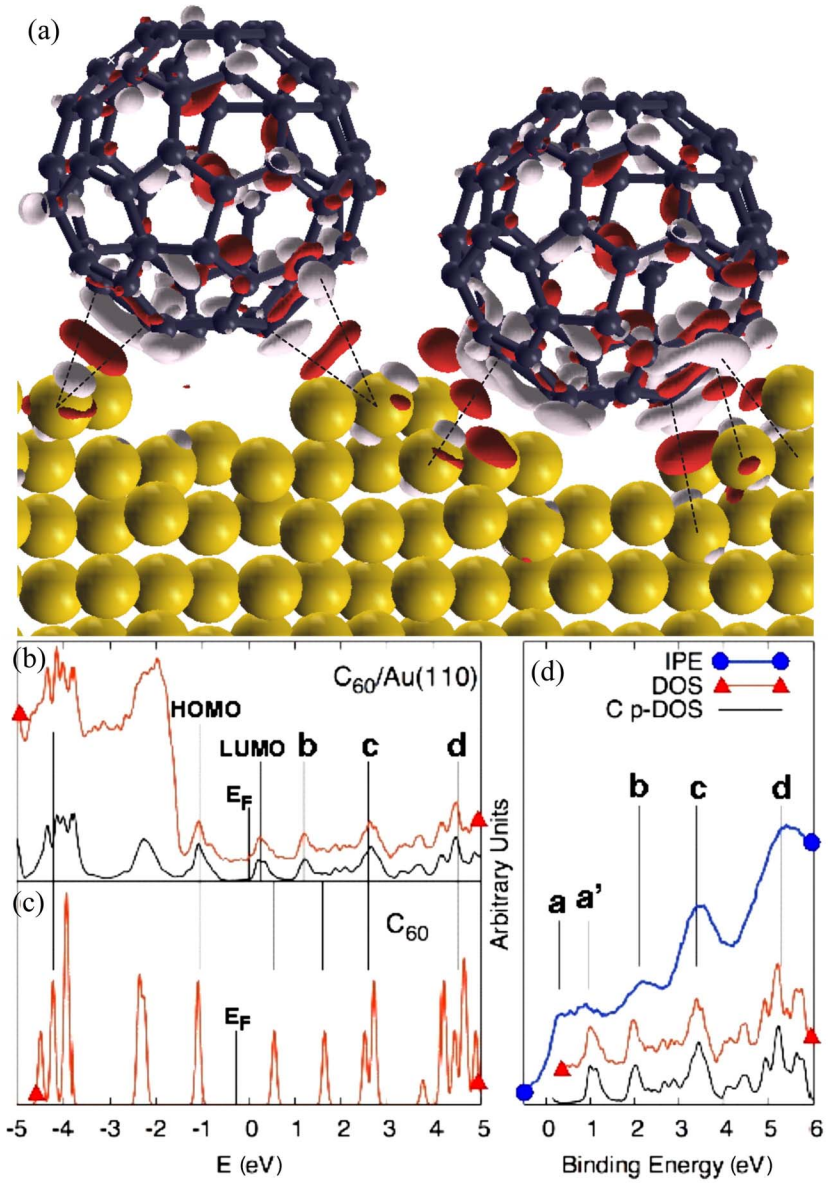

FIG. 3. (Color online) (a) Bonding charge density obtained from DFT calculation of the structure model shown in Fig. 1(c). Positive and negative electron density isosurfaces ($|0.005|$ e/Å^3) are displayed as red (dark gray) and light gray areas, respectively. (b) Experimental PE spectrum (red), calculated DOS (black) for C60/Au(110), and (c) C p-DOS for an isolated C60 molecule. (d) Conduction band IPE data and C p-DOS for C60/(110). PE, IPE, and C p-DOS spectra are displayed as red (up triangles), blue (filled circles), or black (without symbol) lines, respectively.

placements along the surface normal and gradually decrease with surface depth (see Ref. 15 for more structural details). The absolute average atomic distortions $\langle|Z|\rangle$ of the three topmost surface layers along this direction are 0.12(2), 0.12(2), and 0.10(2) Å, respectively, while the [minimum, average, and maximum] bond distortions between the first/second, second/third, and third/fourth layers are [2.62(3), 2.85(2), 3.19(3)], [2.57, 2.86, 3.19], and [2.59, 2.90, 3.17] Å, respectively.[22] Figure 2: (a) Comparison between experimental and calculated in-plane data corresponding to the C60/Au(110)-$p(6\times5)$ surface reconstruction. The measured values and their associated uncertainties are proportional to the radii of the two empty semicircles. The filled semicircles are proportional to calculated values obtained from the final structure shown in Fig. 1(c). Figure 2: (b) and (c) show several experimental (points) and calculated (continuous lines) data corresponding to FORs and CTRs obtained from the final structure. The values close to the curves indicate their corresponding offset for a better visualization.

DFT calculations based on plane waves, pseudopotentials, and periodic supercells[15,23–25] were able to elucidate the molecular bonding mechanism, which induces the nanopit formation in the reconstructed Au(110) surface. The electronic ground state was calculated for the local geometry of the C60 adsorbed in the Au nanopits, which results from the SXRD analysis. The calculated bonding charge, the density of electronic states (DOS), and the partial DOS (C p-DOS, which results from projecting the wave functions on the atomic C 2p states) provide evidence of strong directional C-Au bonding (Fig. 3).

The bonding charge density is mostly localized between the lateral C atoms in contact with the nanodimple edges, while the interstitial region directly underneath the C60 is not primarily involved in bond formation. The degree of directional electronic contribution to bonding is showed in Fig. 3(a) by charge accumulation (red areas) localized along the shortest C-Au bond lengths (marked by dashed lines and ranging between 3.1 and 3.3 Å). Moreover, molecular adsorption induces the polarization of the C60, involving

mostly the C atoms on the lower half of the molecule. These results confirm the directional character of the interfacial C-Au bonding proposed by Wang and Chen[26] for C60 on the unreconstructed Au(111) surface and by Baxter *et al.*[22] for C60 on the (6×5) reconstructed Au(110) surface on the basis of DFT and classical molecular dynamics calculations, respectively.

Any ionic contribution to the C60/Au(110) bonding would result in new molecular features at the Fermi level due to the population of the C60 lowest unoccupied molecular orbital (LUMO), as those measured in the C60/Ag and C60/Cu systems.[27,28] In the present case, both the PE spectrum[29] and the calculated DOS [Fig. 3(b)] do not present any new feature between the Fermi level and the C60 highest occupied molecular orbital (HOMO). The same conclusion can be drawn from the analysis of the unoccupied states [conduction band inverse photoemission data,[8] IPE, and DOS in Figs. 3(b) and 3(c)]. With respect to an isolated C60 molecule [Fig. 3(c)], the LUMO and LUMO+1 states (labeled *b*) are shifted to lower energies upon adsorption [Fig. 3(b)] but no sizable fraction of the C60 LUMO is transferred below the Fermi level. Moreover, the HOMO and the higher energy molecular states [labeled *c* and *d* in Figs. 3(b) and 3(c)] are not affected by the adsorption. This allows us to align the calculated energies of the *c* and *d* states to the corresponding features in the IPE [Fig. 3(d)]. By doing so, we conclude that the broad feature above to the Fermi level (*a* and *a'*) results from two different origins: a flat contribution from the gold *s* states (*a*) and the molecular LUMO (*a'*). At higher energies, the spectrum is dominated by the three distinct molecular peaks [*b*, *c*, and *d* in Fig. 3(d)].

The additional charge available after C60 adsorption is redistributed in the contact interfacial region, and substrate mass transport takes place to form and maximize the number of strong directional bonds. In fcc metals, the hexagonal structure of (111) surfaces allows the formation of 12 C-metal bonds by surface vacancy formation, as for C60/Pt(111) (Ref. 10) and C60/Al(111).[30] Mass transport is facilitated on more open substrates, such as the Au(110) surface, where nanodimple formation allows us to maximize the number of bonds. In the present case, the measured fullerene corrugation is due to the presence of two different adsorption sites with different heights. The lack of measured corrugation in other systems, as in C60 on Au(111) or Cu(110),[29] does not necessarily imply that the C60 is bound to the ideal surface termination. In fact, surface defects could also be formed in these cases but the corrugation might be suppressed by the presence of just one binding site per unit cell.

In conclusion, we have shown that for the C60/Au(110) 6×5 system, the development of strong directional bonding between π molecular orbitals and *s* metal electrons of the topmost surface gold atoms induces the formation of nanoscopic dimples, which hosts the fullerene molecules. The linking between the redistribution of bonds observed from spectroscopy data analysis and bonding directionality is established via DFT calculations performed on the interface structure determined from the diffraction data. These results have implications on the adsorption of LMs on metal surfaces and could lead to the revision of some interaction mechanisms determined by the STM analysis.

X.T. and J.R. thank the Spanish M.E.C. Agency for partially funding this project through Project No. MAT2005-01736. P. Rudolf is acknowledged for fruitful discussions. S. Nannarone and S. Baroni are kindly acknowledged for discussions and encouragement.

*Author to whom correspondence should be addressed. xavier@icmab.es

[1] P. Leclere *et al.*, Mater. Sci. Eng., R. **55**, 1 (2007).
[2] F. Rosei, M. Schunack, and Y. Naitoh, Prog. Surf. Sci. **71**, 95 (2003).
[3] M. Pedio *et al.*, Phys. Rev. Lett. **85**, 1040 (2000).
[4] X. Lu *et al.*, Phys. Rev. Lett. **90**, 096802 (2003).
[5] P. Rudolf, G. Gensterblum, and R. Caudano, J. Phys. IV **7**, 137 (1997).
[6] D. N. Futaba and S. Chiang, Jpn. J. Appl. Phys., Part 1 **38**, 3809 (1999).
[7] X. Lu *et al.*, Phys. Rev. B **70**, 115418 (2004).
[8] I. K. Robinson and D. J. Tweet, Rep. Prog. Phys. **55**, 599 (1992).
[9] R. Feidenhans'l, Surf. Sci. Rep. **10**, 105 (1989).
[10] R. Felici, M. Pedio, and F. Borgatti, Nat. Mater. **4**, 688 (2005).
[11] V. Langlais, X. Torrelles, Y. Gauthier, and M. De Santis, Phys. Rev. B **76**, 035433 (2007).
[12] X. Torrelles *et al.*, ESRF Newsletter **39**, 17 (2004).
[13] S. Modesti, S. Cerasari, and P. Rudolf, Phys. Rev. Lett. **71**, 2469 (1993).
[14] W. W. Pai *et al.*, Phys. Rev. B **69**, 125405 (2004).
[15] See EPAPS Document No. E-PRBMDO-77-078815 for access to further information on sample preparation, structural details of C60/Au(110)-$p(6\times5)$ superstructure, and the theoretical DFT method used. For more information on EPAPS, see http://www.aip.org/pubservs/epaps.html.
[16] M. Pedio *et al.*, J. Electron Spectrosc. Relat. Phenom. **76**, 405 (1995).
[17] A. J. Maxwell *et al.*, Phys. Rev. B **49**, 10717 (1994).
[18] S. Ferrer and F. Comin, Rev. Sci. Instrum. **66**, 1674 (1995).
[19] F. Comin *et al.*, J. Phys. IV **7**, C2/343 (1997).
[20] J. K. Gimzewski, S. Modesti, and R. R. Schlittler, Phys. Rev. Lett. **72**, 1036 (1994).
[21] M. Copel and T. Gustafsson, Phys. Rev. Lett. **57**, 723 (1986).
[22] R. Baxter, P. Rudolf, G. Teobaldi, and F. Zerbetto, ChemPhysChem **5**, 245 (2004).
[23] J. P. Perdew, K. Burke, and M. Ernzerhof, Phys. Rev. Lett. **77**, 3865 (1996).
[24] S. Baroni, A. Dal Corso, S. de Gironcoli, and P. Giannozzi, http://www.pwscf.org/.
[25] D. Vanderbilt, Phys. Rev. B **41**, 7892 (1990).
[26] L.-L. Wang and H.-P. Cheng, Phys. Rev. B **69**, 165417 (2004).
[27] S. J. Chase *et al.*, Phys. Rev. B **46**, 7873 (1992).
[28] Z. H. Lu *et al.*, Phys. Rev. B **72**, 155440 (2005).
[29] P. W. Murray *et al.*, Phys. Rev. B **55**, 9360 (1997).
[30] M. Stengel, A. De Vita, and A. Baldereschi, Phys. Rev. Lett. **91**, 166101 (2003).